VIROLOGY 237, 217–227 (1997)
ARTICLE NO. VY978776

Katherine Monastyrskaya,*,†,[1] Norbert Staeuber,*,†,[2] Geoff Sutton,*,† and Polly Roy*,†,‡,[3]

*Department of Biochemistry, University of Oxford, Oxford, OX1 3QU, United Kingdom; †NERC Institute of Virology and Environmental Microbiology, Mansfield Road, Oxford, OX1 3SR, United Kingdom; and ‡Department of International Health, University of Alabama at Birmingham, Birmingham, Alabama 35294

Received February 26, 1997; returned to author for revision April 18, 1997; accepted August 8, 1997

Based on the crystal structure of the VP7 major core protein of bluetongue virus serotype 10 (BTV-10) and that of the top domain of the VP7 protein of African horsesickness virus serotype 4 (AHSV-4), chimeras and site-directed mutants of the proteins were constructed and the products analyzed with respect to their properties and functions. Chimeras with the central upper domain of BTV-10 VP7 replaced by that of AHSV-4 VP7 (construct BAB) formed trimers, as did the converse construct (ABA). Further, both proteins exhibited the expected conformational epitopes of the constituent sequences. Using BAB VP7 it was demonstrated that residues of the upper domain of AHSV-4 VP7 contribute to the observed insolubility of the protein. By contrast, ABA VP7 protein was as soluble as wild-type BTV-10 VP7. Replacement of selected amino acid residues in the top domain (e.g., A167 by R; F209 by T) improved the solubility of BAB VP7. Since the trimeric BAB and ABA VP7 proteins did not form core-like particles (CLPs) when coexpressed with BTV VP3, it was concluded that trimerization of chimeric VP7 is not sufficient for CLP formation. When the N-terminal region of the ABA protein (aa 1–120) was replaced by the respective sequences of BTV VP7 (construct BBA), the protein aggregated and did not form CLPs with coexpressed BTV VP3, most likely due to disruption of the required contacts between the N- and C-terminal regions of the bottom domain, leading to incorrect folding of the chimera.

INTRODUCTION

Orbiviruses (family *Reoviridae*) have virions consisting of nonenveloped particles (86 nm in diameter) that encapsulate the 10-segment, double-stranded, RNA genome. Among the recognized orbiviruses, bluetongue virus (BTV), the prototype orbivirus, the related African horsesickness virus (AHSV), and epizootic hemorrhagic disease virus (EHDV), are transmitted by species of gnats and infect certain wild and domestic (livestock) vertebrates with occasional high morbidity and mortality (Murphy *et al.,* 1971). Virions of these viruses have four major structural proteins (VP2, VP3, VP5, and VP7; Roy, 1996a,b). Recent advances in understanding the macromolecular organization of BTV have come from studies involving cryoelectron microscopy (cryo-EM) of baculovirus-expressed BTV core-like particles (CLPs), and virus-like particles (VLPs), as well as from virus-derived cores (Hewat *et al.,* 1992a,b; Prasad *et al.,* 1992). The BTV-10 VP7 protein (38 kDa) is a major constituent of the virus core with, per particle, 780 molecules arranged as 260 trimers and forming a T = 13 *l* lattice (Grimes *et al.,* 1995) that overlays a subcore whose principal component is the VP3 protein (120 monomers, 60 dimers; D. Stuart, unpublished data). VP7 also interacts with the two outer capsid proteins, VP2 and VP5 (Hewat *et al.,* 1992b). In addition, there are VP7 trimer–trimer interactions in the core, most likely involving the VP7 carboxy termini which extend out of the side of the trimer arrangement. At the amino acid (aa) sequence level, BTV-10 VP7 protein is highly conserved among BTV serotypes (>95% sequence identity, depending on the serotype) and closely related to the VP7 proteins of AHSV and EHDV (Iwata *et al.,* 1992a,b).

Although the BTV VP7 molecules contain a high percentage of hydrophobic residues, BTV-10 VP7 synthesized by recombinant baculoviruses is soluble and, under the appropriate conditions, forms crystals of VP7 trimers (Basak *et al.,* 1992). This property has allowed the 3-dimensional structure of VP7 to be determined to a resolution of 2.6 Å (Grimes *et al.,* 1995). Similarly, the upper domain of the AHSV-4 VP7 has been determined (Basak *et al.,* 1996). From these data it has been shown that the VP7 monomer is composed of two distinct domains (Fig. 1A). The upper domain is formed by the central one-third of the polypeptide chain (aa 121–249), folded into an antiparallel β-sandwich. The lower domain contains the N-terminal region composed of 5 α-helices (aa 1–120) and four C-terminal α-helices (aa 250–349) that together form a bundle of nine helices with loops

[1] Present address: Givaudan Roure Forschung AG, Ueberlandstrasse 138, CH-8600 Duebendorf, Switzerland.

[2] Present address: Institute of Virology, Veterinary Faculty, University of Zurich, Winterthurerstrasse 266a, CH-8057 Zurich, Switzerland.

[3] To whom correspondence and reprint requests should be addressed at NERC Institute of Virology and Environmental Microbiology, Mansfield Road, Oxford, OX1 3SR, UK. Fax: ++44 1865 559962. E-mail: por@mail.nerc-oxford.ac.uk.

0042-6822/97 $25.00

in-between (Fig. 1A). The two domains are twisted anticlockwise in the trimer so that the top domain of one monomer rests on the lower domain of the threefold related subunit, primarily the C-terminal region.

In contrast to BTV, the AHSV VP7 forms flat hexagonal crystals in the cytoplasm of infected cells (Burroughs *et al.,* 1994) and, likewise, large disc-shaped crystals when expressed by a recombinant baculovirus (Chuma *et al.,* 1992). Due to this intrinsic insolubility, purification of a soluble form of the complete AHSV-4 VP7 has proved difficult and only the top domain has been crystallized (Basak *et al.,* 1996). The X-ray structure of this top domain is very similar to that of the upper domain of BTV VP7 trimers, as expected from the high degree of sequence similarity of the BTV and AHSV VP7 proteins (overall: 67% similarity, 46% identity). Despite this, it has not been possible to substitute AHSV VP7 for BTV VP7 in the formation of chimeric CLPs using baculovirus-expressed BTV VP3 and AHSV VP7 proteins (unpublished data). By contrast, when EHDV-1 VP7 was coexpressed with BTV VP3, chimeric CLPs were formed (unpublished data; Le Blois *et al.,* 1991). EHDV-1 VP7 exhibits a 81% similarity and 64% identity with BTV-10 VP7 (Iwata *et al.,* 1992a).

Using the available molecular and structural information for BTV and AHSV VP7 proteins, we have exchanged specific regions and domains of the VP7 proteins of BTV and AHSV and determined the effects on protein solubility, folding, trimerization, and the ability to form CLPs with BTV VP3 protein. Further, the effects of replacing specific aa of the AHSV VP7 (and BAB) protein by their counterparts from BTV VP7 were investigated. The mutant proteins were expressed from the derived recombinant baculoviruses. Some improvement in solubility was identified in the mutant BAB protein, but none for the mutant AHSV protein.

MATERIALS AND METHODS

Viruses and cells

S. frugiperda (Sf) cells were grown in suspension and monolayer cultures at 28° in TC100 medium supplemented with 10% (v/v) fetal calf serum. Derivatives of *Autographa californica* nuclear polyhedrosis virus (AcNPV) containing the wild-type BTV-10 VP7 gene (Ac10BTV7; Oldfield *et al.,* 1990), or that of AHSV-4 (Ac4AHSV7; Chuma *et al.,* 1992), and the various VP7 mutants that were constructed, were plaque purified and propagated as described elsewhere (Brown and Faulkner, 1977; King and Possee, 1992).

Construction of recombinant transfer vectors and baculovirus expression vectors to synthesize chimeric BAB, ABA, BBA VP7, and ABB proteins

For the BAB construct, PCR was employed to construct a chimeric VP7 gene encoding (in order) BTV-10 VP7 aa residues 1 to 120 (representing the bottom domain N-terminal α-helical region), aa residues 121 to 249 of AHSV VP7 (the β-sheet region of the top domain) and aa 250 to 349 of BTV VP7 (the C-terminal α-helical region of the bottom domain). To amplify each bottom domain region of BTV-10 VP7, the plasmid transfer vector pAc10BTV7 DNA (Oldfield *et al.,* 1990) was used as template. This plasmid contains the BTV-10 VP7 gene inserted into a unique *Bam*HI site in the parent transfer vector pAcYM1 (Matsuura *et al.,* 1987). Two pairs of primers were used (Table 1), a forward primer, Bac 1, together with the reverse primer BT1, and the forward primer BT4 together with the reverse primer Bac 2. The forward primer Bac 1 corresponded to an AcNPV sequence upstream of the BTV-10 VP7 gene in the plasmid. The back primer, Bac 2, corresponded to a region of the AcNPV genome some 60 nucleotides downstream of the VP7 insertion site in the plasmid and represents a sequence of the complementary, noncoding DNA strand. The primers BT1 and BT4 each contain a *Fok*I recognition site (underlined in Table 1) and sequences that, for BT1, corresponded to the complementary strand residues 381–367 of the VP7 gene and, for BT4, the coding strand residues 756–774. *Vent* DNA polymerase (New England Biolabs) was used for the PCR amplifications. The amplified products were treated with proteinase K, extracted with phenol, digested with *Bam*HI and *Fok*I, and purified using a QIAEX II Gel Extraction kit as described by the manufacturer (Qiagen). The purified products were employed for the subsequent cloning procedures. The sequences encoding the top domain of AHSV-4 VP7 were amplified using, as template, the plasmid transfer vector pAc4AHSV7 (Chuma *et al.,* 1992) and the forward primer AH2 (corresponding to residues 360–381 of the AHSV VP7 coding sequence), and the reverse primer AH3

TABLE 1

Oligonucleotide Primers Used in PCR Reactions

Name	Nucleotide sequence
Bac 1	5′-TGATAACCATCTCGCAA-3′
Bac 2	5′-CGCACAGAATCTAGCGC-3′
BT1	5′-GGCCGGATG*CTGGCCCCCATGTGC*-3′
BT4	5′-GGCCGGATG*GTTGTGTTCTATATACTA*-3′
AH2	5′-GGCCGGATG*CAAATGCAAACATTCGGACCAA*-3′
AH3	5′-GGCCGGATG*CCAAAGACGTATACCATAA*-3′
RVD	5′-ACTGGAAATGTCTATCA-3′
AH-Sma	5′-CGCGCCCCGGG*TCCGAATGTTTGCATTTG*-3′
AH-Spe	5′-CGCGCACTAGT*TTGGATAGATCGCTAGAC*-3′
BT-Sma	5′-CGC5′GCCCCGGG*CGTCAGCCTTATGGTTT*-3′
BT-Spe	5′-CCGCGACTAGT*ATAGAACACAACCTGTATTTG*-3′
APvuF	5′-GGGGCGATCG*CTAGACACGGTT*-3′
BPvuR	5′-GGGGCGATCG*ATCCATAGATATATAAAG*-3′

*Note. Fok*I, *Spe*I, *Sma*I, and *Pvu*I cloning sites are underlined. In oligonucleotide primers BT1, BT4, AH2, AH3, AH-Sma, AH-Spe, BT-Sma, BT-Spe, APvuF, and BPvuR the sequences corresponding or complementary to the BTV-10 and AHSV-4 VP7 genes are shown in italics.

(corresponding to the complement of residues 777–759 of the AHSV-4 VP7 gene). As in the case of the BTV gene, pAc4AHSV7 consisted of a copy of the AHSV-4 VP7 gene inserted into the transfer vector pAcYM1. Following PCR amplification and purification of the product, the AHSV VP7 gene fragment was digested with *Fok*I, then ligated into pAcYM1 (previously purified following digestion with *Bam*HI) together with the appropriately digested BTV-10 VP7 lower domain gene fragments, to form the recombinant transfer vector. Clones of the resulting construct, pAcBAB7, were confirmed by sequence analyses (Sanger *et al.,* 1977) to have the expected chimeric VP7 arrangement (BAB) as shown in schematic form in Fig. 1B.

The chimeric ABA and BBA VP7 genes were constructed similarly. For ABA, two pairs of primers were employed to amplify (by PCR) the N- and C-terminal regions of AHSV VP7. These were the forward primer RVD together with the reverse primer AH-Sma, as well as the forward primer AH-Spe and the reverse primer Bac 2 (Table 1). The RVD primer corresponded to the AcNPV sequence in the transfer vector that is upstream of the unique *Eco*RV site, while the reverse AH-Sma primer represented the sequence complementary to the VP7 coding residues 377–360. To facilitate subsequent manipulations, the AH-Sma primer contained a downstream *Sma*I restriction enzyme site (Table 1). The AH-Spe forward primer corresponded to AHSV VP7 coding residues 774–791 and contained an *Spe*I restriction site to facilitate subsequent manipulations (Table 1). As before, following PCR amplification the products were purified and digested with the appropriate enzymes (*Eco*RV, *Sma*I, *Spe*I) for subsequent construction of the chimeric gene. Similarly, the top domain sequences of the BTV VP7 gene were amplified using the forward BT-Sma primer, which corresponded to the coding residues 384–400, and the reverse BT-Spe primer that was complementary to residues 767–747 of the BTV VP7 gene. Each primer provided a restriction enzyme site for cloning purposes (*Sma*I and *Spe*I, respectively). Following PCR amplification and purification, the fragments were digested with the appropriate restriction endonucleases. To form the chimera, and since the recombinant transfer vector pAc4AHSV7 has internal *Bam*HI and *Spe*I sites (Chuma *et al.,* 1992), it was initially digested with *Eco*RV and *Spe*I and the linearized product recovered and ligated to the amplified PCR fragments (previously digested with *Eco*RV, *Sma*I, and *Spe*I prior to purification and ligation). The resulting recombinant transfer vectors were characterized and one, pAcABA7, was selected and confirmed by sequence analyses to have the appropriate arrangement (see Fig. 1C).

For BBA VP7, the sequences encoding aa 1–249 of BTV-10 VP7 (the first five helices of the bottom domain plus the whole of the top domain) were amplified using Bac 1 and the reverse primer BPvuR (Table 1) which contained a flanking *Pvu*I site. The BPvuR primer contained sequences complementary to BTV-10 VP7 coding residues 797–786. The sequence encoding AHSV-4 VP7 aa 250–350 was amplified by PCR using, as template, pAc4AHSV7 (Chuma *et al.,* 1992) and the forward primer APvuF (containing a unique *Pvu*I site), and reverse primer Bac 2. The APvuF primer contained sequences corresponding to AHSV VP7 coding residues 761–779. The two PCR products were digested with *Pvu*I and *Bam*HI, the products purified and cloned into pAcYM1 (previously digested with *Bam*HI and purified prior to ligation). A recombinant plasmid, pAcBBA7, with the correct VP7 arrangement (see Fig. 1D) was recovered and characterized by sequence analyses (Sanger *et al.,* 1977). The ABB (see Fig. 1E) construct, which consists of the N-terminal α-helix region of AHSV-VP7 and the remaining sequences of BTV VP7 was similarly generated using the forward primer RVD together with the reverse primer AH-Sma (see Fig. 1E), as well as the forward primer BT-Sma and the reverse primer Bac2 (Table 1). The recombinant plasmid, pAcABB7, was characterized as described above.

Transfection and selection of recombinant baculoviruses

The lipofection technique (Felgner *et al.,* 1987) was used to cotransfect monolayers of Sf cells with recombinant transfer vectors using *Bsu*36I triple-cut AcNPV DNA (Kitts and Possee, 1993). Recombinant baculoviruses were initially selected on the basis of their *lac*Z-negative phenotypes, plaque purified, and propagated to high titers as described elsewhere (King and Possee, 1992). The transfer vectors pAcBAB7, pAcABA7, pAcBBA7, and pAcABB7 were used to generate the recombinant baculoviruses AcBAB7, AcABA7, AcBBA7, and AcABB7.

Site-directed mutagenesis, construction of transfer vectors and isolation of recombinant baculoviruses expressing other mutant VP7 proteins

Using the single-strand capacity of the baculovirus transfer vector pAcCL29 (Livingstone and Jones, 1989), synthetic oligonucleotides were employed to prepare specific VP7 mutants by the method described by Kunkel and associates (1987). For templates, the wild-type AHSV-4 VP7 gene and the recombinant BAB VP7 gene were recovered from the respective transfer vectors, pAc4AHSV7 and pAcBAB7, by excision with *Bam*HI and subcloned into the *Bam*HI site of pAcCL29. Two oligonucleotides were employed for mutagenesis of these genes: A167R (5′-GACCTGTCCTCTAGCGCCTGC-3′), which was used to replace the AHSV VP7 alanine at residue 167 (A167) by arginine (A167R), and F209T (5′-AACGGTGACAGTAGTCCCTGG-3′), which was used to replace the AHSV VP7 phenylalanine at residue 209 (F209) by threonine (F209T). [The AHSV sequences refer to the corrected sequence as deduced from the crystallographic data of the AHSV VP7 upper domain reported by

Basak and colleagues (1996), rather than the previously published VP7 sequence (see Iwata *et al.,* 1992a).] In these sequences the mutated anticodons are underlined. Both oligonucleotides represented the complement of the coding strand of the AHSV gene. The recombinant transfer vectors were recovered and the mutated sequences confirmed by sequence analyses. Using these recombinant transfer vectors, the recombinant baculoviruses AcAHSV7-A167R, AcAHSV7-F209T, AcBAB7-A167R, and AcBAB7-F209T were isolated as described above.

Solubility assays and purification of recombinant VP7 protein by ammonium sulfate precipitation

Infected Sf cells were harvested 72 hr postinfection, washed in PBS, resuspended in cold TNN buffer (200 m*M* Tris–HCl, pH 8.0, 150 m*M* NaCl, 0.5% Nonidet P-40), and homogenized at 4°. Cell debris and nuclei were then pelleted by centrifugation (5 min at 2,500 *g*). As required, ice-cold, saturated ammonium sulfate in 100 m*M* Tris–HCl, pH 7.5, was added to the cytoplasmic cell extracts to provide a final concentration of 20% v/v. The precipitated protein was pelleted by centrifugation and resuspended in 10 m*M* Tris–HCl, pH 7.5, and dialyzed against the same buffer at 4° overnight. Insoluble material was removed by pelleting at 18,000 *g* for 10 min, and the soluble VP7 was stored at −20° until required.

SDS–polyacrylamide gel electrophoresis (SDS–PAGE) and Western blot analysis

Sf cell monolayers were infected with a recombinant baculovirus using a m.o.i. of 5–10 PFU per cell (French and Roy, 1990). Cells were harvested at 72 hr postinfection, washed with PBS, and lysed at 4° in TNN. Samples were then suspended in protein dissociation buffer (10% (v/v) β-mercaptoethanol, 10% (w/v) SDS, 25% (v/v) glycerol, 10 m*M* Tris–HCl, pH 6.8, and 0.02% (w/v) bromophenol blue) and either heated at 37°, or boiled at 100°, for 10 min and the products subsequently resolved by 10% SDS–PAGE, followed by staining with Coomassie brilliant blue. For Western blot analysis, proteins from gels were transferred onto a PVDF membrane by standard blotting procedures. Membranes containing protein were incubated with the specified antiserum diluted 1:1000 in blocking buffer (5% (w/v) skimmed milk, 0.05% (v/v) Tween-20 in PBS), followed by incubation with the secondary antibody conjugated with alkaline phosphatase, and the bound products were identified using the alkaline phosphatase substrate NBT-BCIP (GIBCO-BRL) in 0.1 *M* Tris–HCl, pH 8.5, 0.1 *M* NaCl, and 0.05 *M* $MgCl_2$.

Enzyme-linked immunosorbent assay (ELISA)

Conventional ELISA procedures were performed as described elsewhere (Gould *et al.,* 1985). In brief, Micro-ELISA plates (Nunc) were coated overnight with an optimal concentration of antigen (10 μg/well for purified protein preparation and approximately 20 μg/well for partially purified protein preparation) in carbonate coating buffer (15 m*M* Na_2CO_3, 36 m*M* $NaHCO_3$, pH 9.6) and subsequently blocked with PBS containing 2% (w/v) skimmed milk. For ELISA using wild-type recombinant BTV and AHSV VP7 as well as chimeric ABA antigen proteins were purified in homogeneity as described above. For insoluble antigen such as BAB, a semipurified concentrated protein obtained after partial solubilization (as described above) or resuspension of the pellet fraction were used. Mouse monoclonal antibodies (MAbs) were raised to purified BTV-10 VP7 and characterized by standard procedures (Kimura-Kuroda and Yasui, 1983). Mouse MAbs raised to purified AHSV-4 VP7 were kindly provided by Drs. I. Casal and J. Martinez-Torrecuadrada (Ingenasa, Spain). Standard procedures of incubation of the primary antibody in serial two- or fivefold dilutions were followed by addition of the alkaline phosphatase-conjugated secondary antibody (anti-mouse IgG, obtained from Sigma, and diluted 1:500 in PBS). The reaction was developed by addition of the enzyme substrate (1 mg/ml of disodium ρ-nitrophenyl phosphate, pNPP, (Sigma) prepared in 100 m*M* glycine, 1 m*M* $MgCl_2$, and 1 m*M* $ZnCl_2$, pH 10.4). The reaction was stopped by addition of 3 *N* NaOH and the optical densities read at 405 nm using samples lacking the primary antibody as controls.

CLP analyses

Cell extracts from coinfections involving recombinant baculoviruses that expressed BTV VP3 and those that expressed BTV VP7, or the mutant VP7 proteins, were analyzed for the presence of CLPs by gradient centrifugation as described by French and Roy (1990). CLPs were examined by electron microscopy after resuspension in 10 m*M* Tris–HCl, pH 7.5, and absorption on to a carbon-coated copper 400 mesh EM grid for 2–3 min, followed by a dH_2O wash and negative staining with 2% (w/v) uranyl acetate. Grids were examined at 100 kV in a JEOL 100CX electron microscope under low dose conditions.

RESULTS

Domain replacement between BTV-10 and AHSV-4 VP7 proteins and construction of chimeric BAB VP7

Sequence analyses of the genes encoding the four major structural proteins (VP2, VP3, VP5, VP7) of BTV-10, EHDV-1, and AHSV-4 have revealed that the BTV and EHDV genes are more closely related than either is to those of AHSV (Roy *et al.,* 1991; Iwata *et al.,* 1992a,b). Nevertheless crystallographic analyses have shown that the top domains of BTV and AHSV VP7 proteins are trimeric and structurally similar (Grimes *et al.,* 1995; Basak *et al.,* 1996). In the AHSV and BTV VP7 top domains, the two proteins exhibit some 29% aa identity and 51% aa homology when one considers aa of similar character.

Only the structure of the top domain of AHSV-4 VP7 is known (Basak *et al.,* 1996). For the bottom domains, sequence comparisons between the BTV and AHSV VP7 proteins (Iwata *et al.,* 1992a,b) indicate that the proteins are more similar (some 65% identity and 82% similarity in the N terminal region; 42% identity and 61% homology in the C-terminal region).

To examine the structural and functional relationships of the BTV and AHSV VP7 proteins, a chimeric protein was constructed containing the bottom domain of BTV and the top domain of AHSV VP7. The chimera, designated BAB VP7, is shown in schematic form in Fig. 1B, including the junction BTV and AHSV sequences. The recombinant protein was expressed in insect cells from a recombinant baculovirus, AcBAB7, giving levels of expression and an electrophoretic mobility in SDS–PAGE comparable to those of the wild-type BTV-10 (Fig. 2, lanes 1 and 3). Chimeric BAB VP7, recovered from the pellets following the lysis of AcBAB7-infected cells, was assayed for trimer formation as described previously (Clapp and Patton, 1991). To assay for trimerization, purified wild-type BTV-10 VP7 or chimeric BAB VP7 protein preparations were resuspended in the SDS–PAGE sample buffer, incubated at 37° for 10 min, and the trimers were detected following resolution in 10% SDS–PAGE. To denature trimers, the samples were boiled at 100° for 10 min prior to electrophoresis. Similar to BTV-10 VP7, when samples of BAB VP7 were incubated only at 37° prior to SDS–PAGE, it was observed that the BAB VP7 protein preparations contained trimers in addition to monomers (Fig. 2, lane 2 for BTV-10 VP7, lane 4 for BAB VP7). Upon denaturation by boiling at 100° for 10 min, only monomers were detected (Fig. 2, lane 1 for BTV-10 VP7, lane 3 for BAB VP7). The use of the pellet fractions rather than purified BAB VP7 protein was due to the fact that upon extraction with nonionic detergents (Materials and Methods), and in the absence of urea, the majority of the BAB VP7 protein was found to be insoluble and remained in the pellet after low speed centrifugation (data not shown), similar to the expressed wild-type AHSV-4 VP7. This was in contrast to BTV VP7 where significant amounts of VP7 monomers were recovered in the supernatant fraction as well as in the pellet (data not shown).

As shown in Fig. 3A, the expressed BAB protein did not react in ELISA to any significant extent with six conformation-dependent, anti-BTV VP7 MAbs, all of which map to the top domain (compare the results with the results obtained with the ABA construct, Fig. 3A). In ELISA, BAB VP7 reacted significantly with three of five available anti-AHSV VP7 MAbs (8BH8, 8DF4, 8BD4). These MAbs are specific to AHSV VP7 and do not cross-react with BTV VP7 (Fig. 3B). The expressed BAB protein did not react with MAbs 10AB1 or 10BH9 in ELISA at levels comparable to the results obtained with AHSV-4 VP7 and the chimera ABA VP7 (Fig. 3B, see later). The data suggest that the MAbs 10AB1 and 10BH9 recognize the lower domain of AHSV VP7 while the MAbs 8BH8, 8DF4, and 8BD4 map to the top domain of AHSV VP7.

When the BAB VP7 protein was coexpressed with BTV-17 VP3 protein no CLPs were detected (data not shown), although both proteins were synthesised at high levels, and in control studies the coexpressed BTV VP3 and VP7 proteins gave CLPs (French and Roy, 1990, data not shown), indicating, in the case of the chimeric VP7, that BAB VP7 and BTV VP3 proteins were structurally incompatible, possibly due to the protein insolubility, or the particular conformation of the BAB VP7 protein and its trimers.

Synthesis and analysis of the ABA VP7 chimeric protein

From analyses of the available crystallographic and amino acid sequence data it has been suggested that the distribution of the residues of the top domain may be critical in relation to the observed solubility of the BTV VP7 and lack of observed solubility in the case of AHSV VP7 protein (Basak *et al.,* 1996). To provide information on the potential bottom domain of the AHSV VP7 protein and to study the impact of the top domain residues in protein solubility and suitability of the construct for CLP formation with expressed BTV VP3, initially a chimeric ABA VP7 gene was prepared that combined the top domain of BTV with the bottom domain of AHSV VP7 (see Fig. 1C). The gene was expressed in insect cells using the recombinant baculovirus AcABA7. In this protein, aa residues corresponding to both regions of the α-helical bottom domain originated from AHSV-4 VP7, and residues constituting the top β-sheet domain came from BTV-10 VP7. Interestingly, by SDS–PAGE the ABA VP7 protein exhibited a slightly faster electrophoretic mobility (Fig. 4A, lane 5) than either the BTV (Fig. 4A, lane 1) or AHSV VP7 proteins (Fig. 4A, lane 3). ABA trimers were also detected in the expressed ABA protein preparations (Fig. 4A, lane 6). In ELISA the protein gave strong reactions with the available six conformation-dependent MAbs raised against purified BTV VP7. Based on these data together with the analysis of BTV-10 VP7 mutants (E. Nason, personal communication) it was concluded that these 6 MAbs map to the upper domain of BTV-10 VP7 (see Fig. 3A; compare the data with the results obtained with the BAB protein described above).

In ELISA, the ABA protein also reacted specifically with the anti-AHSV-4 VP7 MAbs 10AB1 and 10BH9 and also with MAb 10AB1 in Western blot analysis (Fig. 4B, lane 3). The ABA chimera did not provide responses in ELISA with MAbs 8BH8, 8DF4, or 8BD4 at levels comparable to the reactions obtained with AHSV-4 VP7, or the BAB chimera (Fig. 3B). Based on these data it was concluded that MAb 10AB1 recognized a linear epitope in the lower domain of AHSV VP7 and that MAb 10BH9 also recognized a lower domain epitope, whereas the other three AHSV MAbs recognized epitopes in the upper domain of the AHSV VP7 protein.

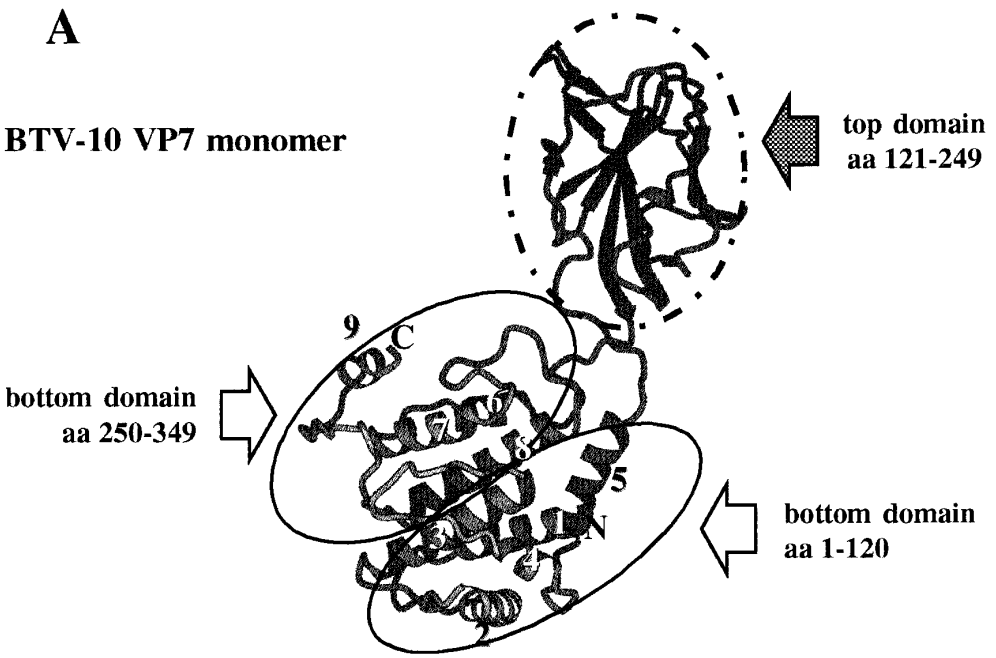
A
BTV-10 VP7 monomer
top domain
aa 121-249
bottom domain
aa 250-349
bottom domain
aa 1-120
9
C
7
10
8
5
3
N
4
1
2

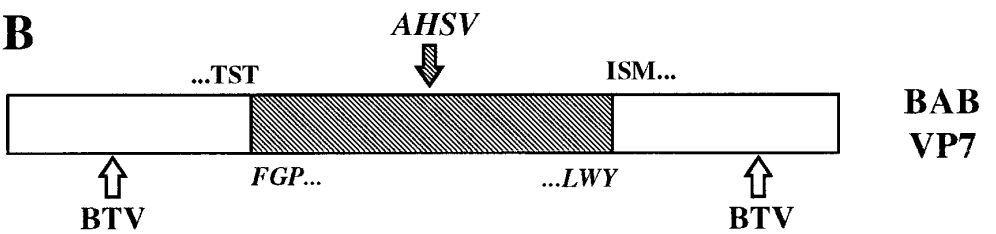
B
AHSV
...TST
ISM...
BAB
VP7
FGP...
...LWY
BTV
BTV

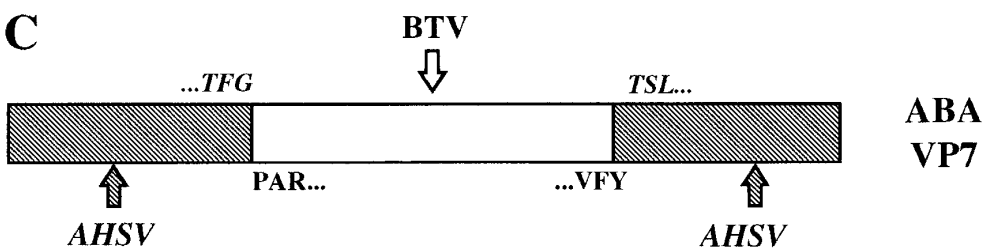
C
BTV
...TFG
TSL...
ABA
VP7
PAR...
...VFY
AHSV
AHSV

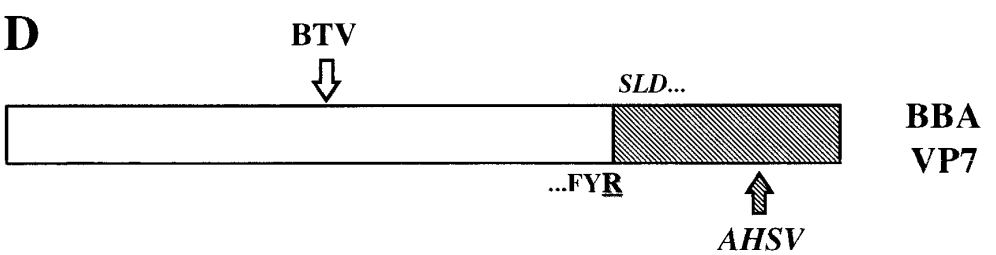
D
BTV
SLD...
BBA
VP7
...FYR
AHSV

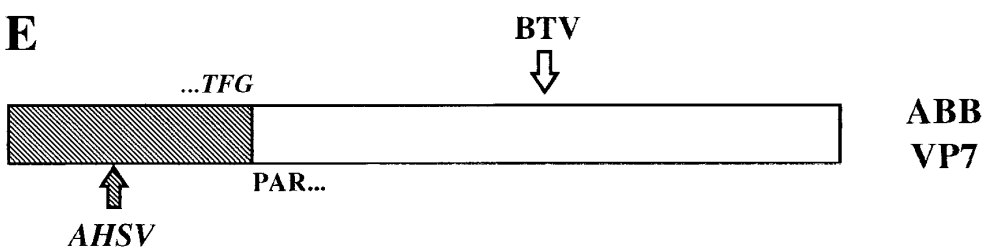
E
BTV
...TFG
ABB
VP7
PAR...
AHSV

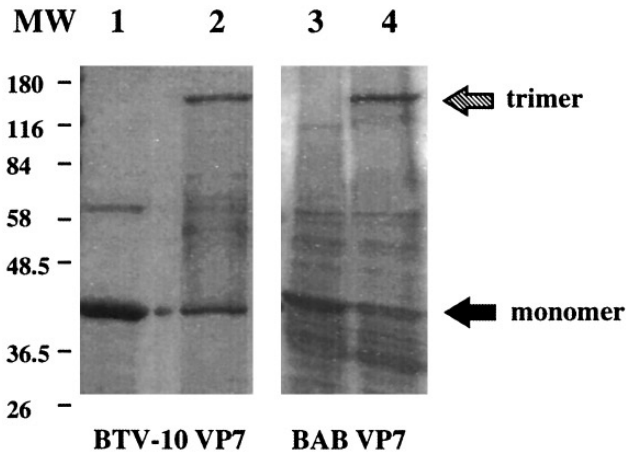

FIG. 2. Expression and trimerisation assays of BTV-10 VP7 and BAB VP7 proteins. The expression of authentic and chimeric proteins recovered from Sf cells infected with the recombinant baculovirus Ac10BTV7 that synthesized wild-type BTV VP7 (lanes 1 and 2) and the recombinant AcBAB7 that produced BAB VP7 (lanes 3 and 4). Lane 1, BTV VP7 following heat denaturation for 10 min at 100°; lane 2, BTV VP7 incubated at 37° prior to SDS–PAGE. In lane 3 is shown the heat denatured (10 min at 100°) chimeric BAB VP7 and in lane 4 BAB VP7, incubated at 37° prior to SDS–PAGE. The positions of the VP7 monomers and trimers are indicated by arrows. Molecular weight markers are shown.

When coexpressed with BTV VP3, the ABA protein failed to produce CLPs as determined by standard assays (French and Roy, 1990, data not shown), indicating that the two proteins were structurally incompatible, possibly due to the particular conformation of the ABA VP7 protein and its trimers.

Synthesis of BBA and ABB VP7 chimeric molecules and analysis of interdomain interactions

The bottom domain of VP7 consists of nine helices and is split in two sections, with four C-terminal helices positioned generally over the five N-terminal helices (see Fig. 1A). To determine whether the BTV N-terminal helices were all that was required for interaction with VP3 in the formation of CLPs and the impact of the helices from different proteins on the trimerization of VP7, a BBA chimeric VP7 gene was constructed. In this construct, the first five N-terminal helices of the ABA chimera were substituted by those of BTV (see Fig. 1D for a schematic of the construct). As indicated in the schematic, and due to the cloning manipulations, an arginine was introduced at the junction site and in lieu of the normal BTV-10 VP7 isoleucine residue (residue 251) or corresponding AHSV-4 VP7 threonine (Iwata *et al.,* 1992a). The BBA VP7 protein was expressed and analyzed for solubility, trimerization, and ability to form CLPs when coexpressed with BTV VP3. Like the BTV or AHSV VP7 proteins, the BBA protein was expressed to high levels and exhibited an identical electrophoretic mobility in SDS–PAGE, but no CLPs were formed on coexpression with BTV VP3 (data not shown). In contrast with the BTV or ABA proteins, but like the AHSV and BAB proteins, essentially all the BBA VP7 was recovered in the pellet after detergent extraction and separation of infected cell lysates by low-speed centrifugation (Fig. 5A, lane 3). However, no trimers were detected in samples that were not boiled prior to SDS–PAGE (data not shown). Surprisingly, the expressed protein did not react with the available, top domain, conformation-dependent anti-BTV-10 VP7 MAbs in ELISA (data not shown), indicating that the conformational epitopes of the upper domain were disrupted and that the chimeric protein had not folded correctly. These results indicate that the amino acid and structural differences between N-terminal helices 1–5 of BTV-10 VP7 and the C-terminal helices 6–9 of AHSV-4 VP7 not only precluded interactions with BTV VP3, but also drastically affected the conformation of the upper domain of the protein. To investigate this further, a second chimeric ABB VP7 was constructed in which the first N-terminal helices represented AHSV VP7, while the remaining molecule represented BTV VP7. The chimeric DNA (see Fig. 1E) was similarly expressed by a recombinant baculovirus and the solubility of the recombinant protein was examined. The protein behaved similarly to that of BBA protein (see Fig. 5B). Although ABB does not possess any mutated residue as in the case of BBA, nevertheless, correct folding was also disrupted and the protein was as insoluble as BBA VP7. As expected, ABB also failed to form CLPs (data not shown).

Replacement of AHSV VP7 Ala 167 by Arg (A167R) or Phe 209 by Thr (F209T) and the effect on the trimerization and solubility of AHSV and chimeric BAB VP7 proteins

In the AHSV-4 VP7 sequence, aa residue 167 is an alanine (A167) while in the comparable sequence of BTV-

FIG. 1. Construction of chimeric BAB, ABA, BBA, and ABB VP7 proteins. (A) A schematic of the arrangement of BTV-10 VP7 is shown (Grimes *et al.,* 1995) in which the two domains of the protein are illustrated: the top β-sheet domain (aa 121–249) and the bottom α-helical domain that is composed of two regions, the N-terminal region, aa 1–120, and the C-terminal region, aa 250–349. The helices of the bottom domain are numbered. In (B) is shown a schematic of the chimeric BAB VP7 protein which consists of the top domain of AHSV-4 VP7 and the bottom domain of BTV-10 VP7. The aa sequences at the junction sites are shown with the BTV sequences above and the AHSV sequences (in italics) shown below the junctions. In (C) is shown a schematic of the chimeric ABA VP7 protein consisting of the top domain of BTV-10 VP7 and the bottom domain of AHSV-4 VP7. The aa sequences at the junctions are provided. In (D) is shown a schematic of the arrangement of a chimeric BBA VP7 consisting of the N-terminal bottom domain region and top domain region of BTV followed by the C-terminal region of the bottom domain of AHSV. The aa sequences at the junction are shown. In this case the BTV VP7 isoleucine at aa 251 (threonine in the comparable AHSV sequence; Iwata *et al.,* 1992a; Basak *et al.,* 1996) was exchanged for an arginine due to the cloning manipulations. In (E) is shown a schematic of the arrangement of a chimeric ABB VP7 consisting of the N-terminal bottom domain region of AHSV, followed by the top domain and C-terminal bottom domain region of BTV. The aa sequences at the junction are shown.

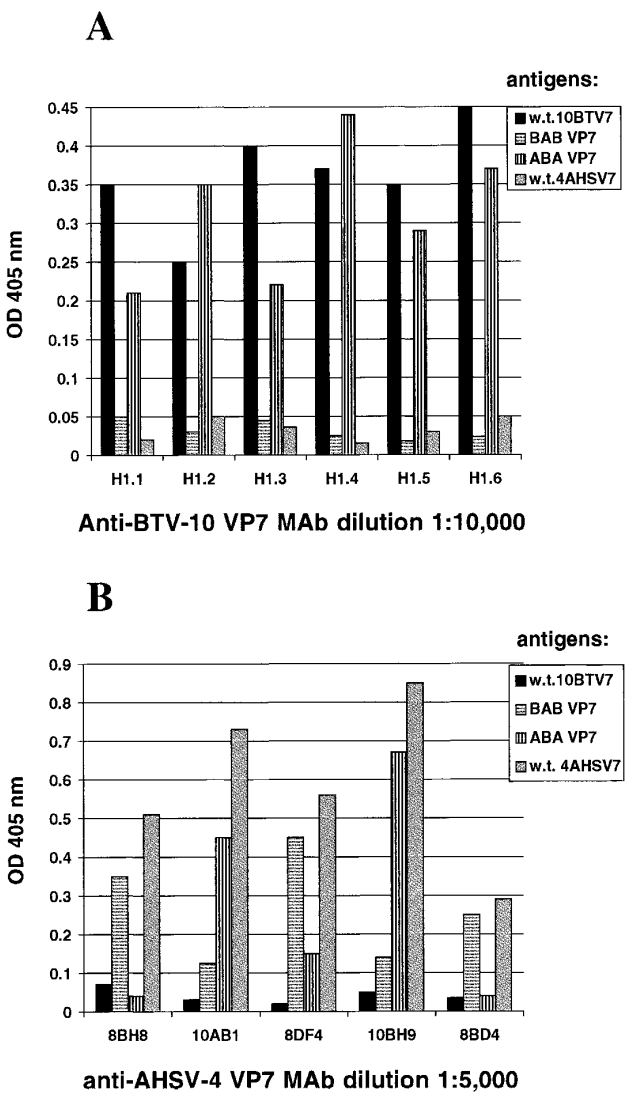

FIG. 3. ELISA analysis of VP7 proteins using anti-BTV-10 or anti-AHSV-4 VP7 MAbs. Micro-ELISA plates were coated with the purified wild-type BTV-10 VP7 (black boxes), or wild-type AHSV-4 VP7 (grey boxes), or recombinant ABA VP7 (boxes with vertical lines), or approximately 20 μg of semipurified recombinant BAB VP7 (boxes with horizontal lines). In (A) a panel of 6 MAbs (H1.1 to H1.6) raised against purified recombinant BTV-10 VP7 was tested with each antigen using 1:1,000 to 1:24,000 dilutions of sera. The OD readings at 405 nm of a 1:10,000 dilution of each MAb are shown. In (B) a panel of 5 MAbs (8BH8, 10AB1, 8DF4, 10BH9, and 8BD4) raised against purified recombinant AHSV-4 VP7 was tested with each antigen using 1:1,000 to 1:10,000 dilutions of sera. The OD readings at 405 nm of a 1:5,000 dilution of each MAb are shown.

10 VP7 it is an arginine (see Iwata *et al.,* 1992a, and Basak *et al.,* 1996). At aa position 209 in the AHSV-4 VP7 there is a phenylalanine, while in the corresponding sequence of BTV-10 VP7 there is a threonine (see Basak *et al.,* 1996). The substitution of A167 and F209 by the aa residues located in equivalent positions in BTV-10 VP7 (R and T) has been suggested as a means to improve the solubility of AHSV-4 VP7 (Basak *et al.,* 1996). To investigate this issue, and to obtain soluble protein for crystallographic purposes, the indicated mutations were carried out as described under Materials and Methods, and the recombinant baculoviruses prepared and used to synthesize the respective proteins, AHSV7-A167R VP7, AHSV7-F209T VP7, BAB7-A167R VP7, and BAB7-F209T VP7.

Both mutations had a stronger effect on the solubility of the chimeric BAB VP7 protein than on AHSV VP7. In fact, neither mutation improved the solubility of AHSV VP7 as evidenced by the observation that the AHSV7-A167R and AHSV7-F209T VP7 proteins were recovered in the pellet fractions following lysis of infected cells in the presence of a nonionic detergent and low speed centrifugation (Figs. 6A and 6B, lane 3). By comparison, some of the mutant BAB7-A167R and BAB7-F209T proteins were recovered in the supernatant (as well as pellet fractions) following cell lysis and low speed centrifugation (Figs. 6C and 6D, lanes 2 and 3). However, based on the relative amounts recovered in the respective pellet and supernatant fractions, the mutant BAB VP7 proteins did not appear to be as soluble as BTV-10 VP7, and little was recovered following ammonium sulfate precipitation. Further in coexpression studies with BTV VP3, none of the mutant proteins formed CLPs with coexpressed BTV VP3 (data not shown).

DISCUSSION

The self-assembly of the BTV VP3 and VP7 proteins into CLPs by coexpression of their genes in insect cells by recombinant baculoviruses (French and Roy, 1990) provides a useful *in vitro* model for studying protein–protein interactions in virus assembly. The crystal structure of BTV-10 VP7 (Grimes *et al.,* 1995) exhibits a β-sandwich structure for the top domain, resembling the jelly roll motif of the influenza virus hemagglutinin and many other viral capsid proteins. The α-helical bottom domain is not commonly observed among viral capsid proteins. The crystallographic data have implicated the lower domain, especially the flat hydrophobic area of helix 2 and adjoining loops at the base of the VP7 trimers, in solving the mismatch that occurs in the interactions of 260 VP7 trimers with a smaller number of underlying VP3 molecules (120 molecules, arranged as dimers) (Burroughs *et al.,* 1995; D. Stuart, personal communication).

A chimeric BAB VP7 protein, combining the top domain of AHSV-4 VP7 with the bottom domain of BTV-10 VP7, was expressed and analyzed for its solubility, antigenic properties, and CLP formation with BTV VP3. It was shown to possess the domain-related antigenic determinants characteristic of the respective BTV and AHSV VP7 proteins, confirming the correct folding of both domains. Similar to AHSV VP7, BAB VP7 formed trimers. However, no CLPs were detected upon coexpression of BAB with BTV VP3, possibly due to its insolubility and tendency to form aggregates. The chimeric protein ABA VP7, possessing the top domain of BTV and the bottom domain of AHSV VP7 also formed trimers and was highly soluble. The fact that ABA VP7 did not form CLPs with BTV VP3

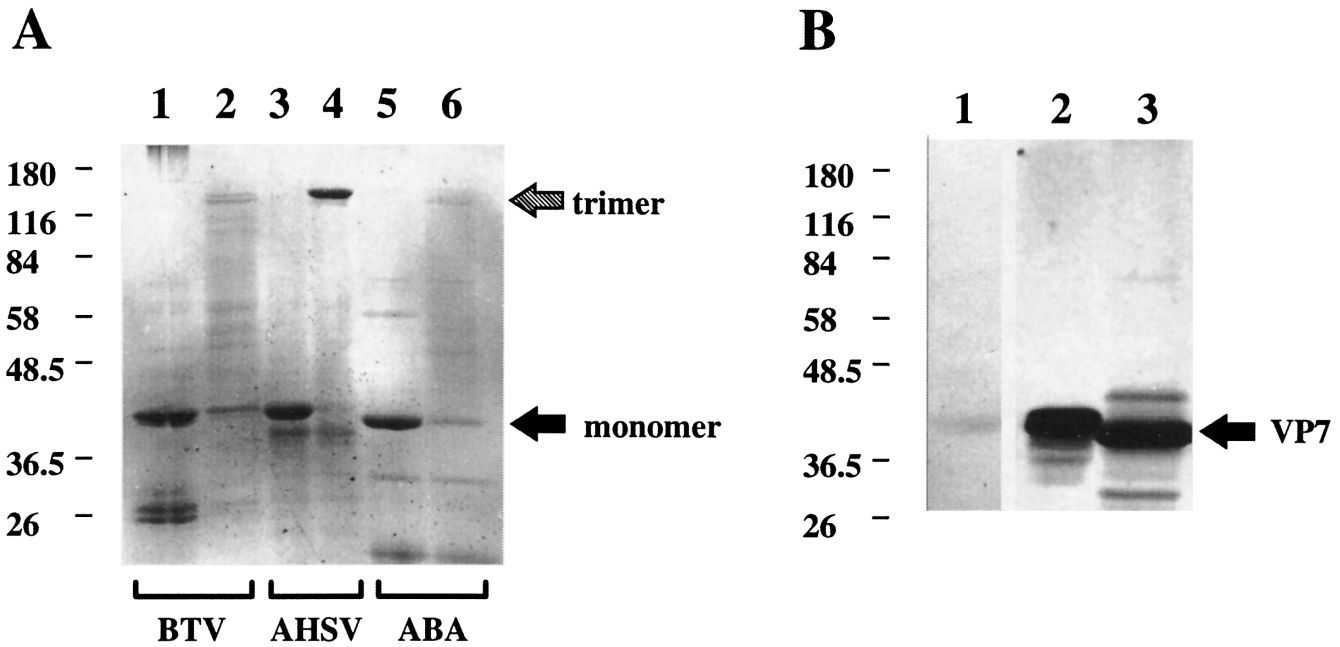

FIG. 4. Expression and characterization of BTV, AHSV, and ABA VP7 proteins. In (A) VP7 proteins were assayed for trimerization, separated by 10% SDS–PAGE, and stained with Coomassie brilliant blue. Lane 1 shows BTV-10 VP7, lane 3 AHSV-4 VP7, and lane 5 the chimeric ABA VP7 protein. All three samples were heat denatured at 100° prior to SDS–PAGE. Lane 2 shows BTV-10 VP7, lane 4 AHSV-4 VP7, and lane 6 the chimeric ABA VP7 protein. The three samples were incubated at 37° prior to SDS–PAGE. In (B) proteins were electroblotted onto membranes and reacted with anti-AHSV-4 VP7 MAb 10AB1 in Western blot analyses. In (B) lane 1 shows the boiled sample of BTV-10 VP7, lane 2 shows the boiled sample of AHSV-4 VP7, lane 3, boiled ABA VP7.

indicates that the aa composition and/or folding of the bottom domain significantly influence the interactions between VP7 trimers and the underlying VP3 scaffold, and that trimerization of VP7 is not by itself a sufficient prerequisite of CLP formation. These findings also support the crystallographic data which have implicated the upper domain in contributing to the insolubility of AHSV-4 VP7. Further, that the α-helical and β-sheet domains of VP7 fold independently involving specific amino acid interactions within the domains. The bottom domain of BTV VP7 is more hydrophobic than the respective area of AHSV-4 VP7 (Basak *et al.,* 1996). The lower part of the bottom domain is composed of the N-terminal helices 1 to 5. Although the amino acid composition of these helices, particularly helix 2, is similar between the two related VP7 proteins, several specific residues likely to contribute to the interactions with the VP3 scaffold are different. Thus alanine (A27) of BTV-10 VP7 is replaced by P in AHSV-4 VP7, V24 by S, N28 by G, L45 by N, G47 by S, T53 by Q, P79 by D. Without the crystal structure of the bottom domain of AHSV-4 VP7 it is difficult to evaluate the precise orientation of these variable residues, however, they might account for the inability of ABA VP7 to form CLPs when coexpressed with BTV VP3.

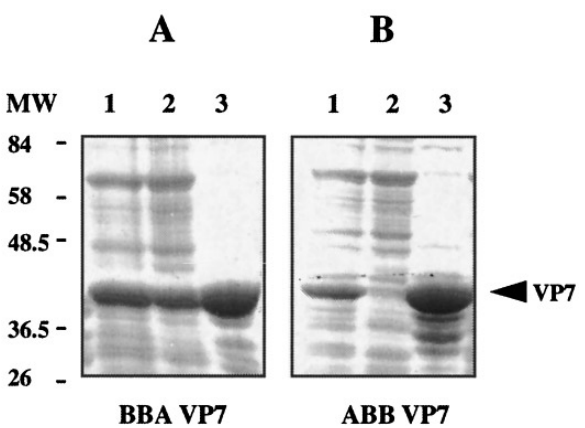

FIG. 5. Solubility assay of the expressed BBA and ABB VP7 proteins. Following lysis in the presence of a nonionic detergent, extracts of Sf cells infected with the AcBBA7 (A) and ACABB7 (B) recombinant baculoviruses were separated by low-speed centrifugation (Materials and Methods). The fractions from each step of purification were resolved by 10% SDS–PAGE and stained with Coomassie brilliant blue. Lane 1 shows the infected cell lysate, lane 2 the supernatant after low-speed centrifugation, and lane 3, the pellet following the low-speed centrifugation of the original extract. The positions of VP7 and molecular weight markers are indicated.

To study the interactions between helices within the bottom domain, the N-terminal α-helices 1 to 5 (aa 1–120) of the ABA chimeric protein, originating from AHSV-4 VP7, were replaced by the respective residues of BTV VP7. The new VP7 chimera, BBA, was expected to possess the bottom surface of BTV VP7. Since none of the residues of the C-terminal part of the lower domain contribute to the base of the trimer, the BBA chimera was expected to interact with BTV VP3 to form CLPs. However, unlike the soluble and trimeric BTV and ABA VP7 proteins, the BBA VP7 was recovered in aggregates fol-

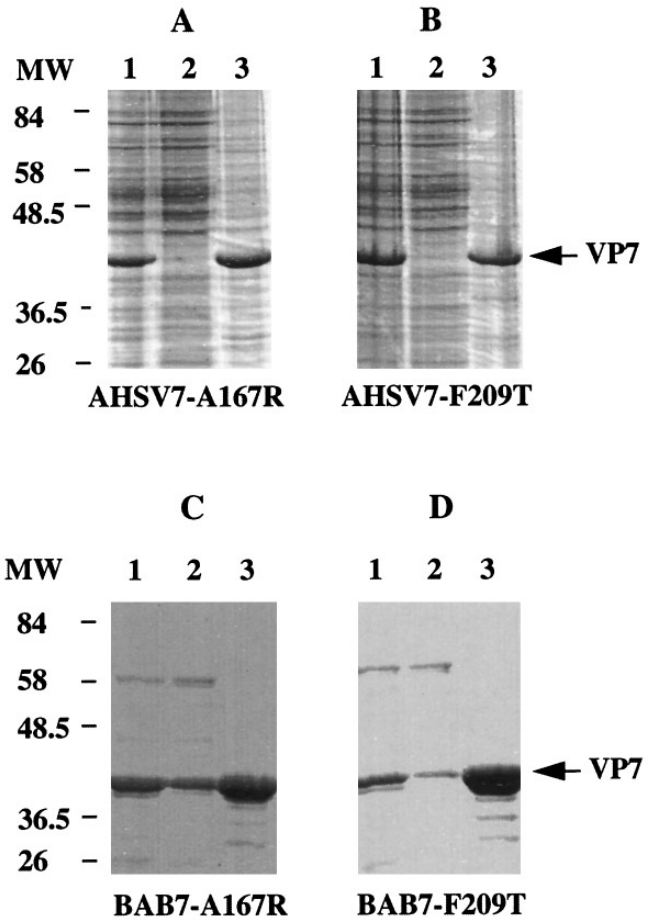

FIG. 6. Solubility assays of AHSV VP7, BAB VP7 mutant proteins. Sf cells were infected with recombinant baculoviruses expressing wild-type or mutant VP7 proteins, lysed in the presence of a nonionic detergent, and fractionated by low-speed centrifugation. Whole cell lysates, supernatant, and pellet fractions were resolved by 10% SDS–PAGE following boiling, then stained either with Coomassie brilliant blue (A and B) or analyzed by Western immunoblotting using polyclonal VP7 antibody (C and D). Whole cell lysates are shown in lane 1, supernatants in lane 2, and pellet fractions in lane 3. (A) AHSV7-A167R; (B) AHSV7-F209T VP7; (C) BAB7-A167R VP7; (D) BAB7-F209T VP7 protein. The positions of VP7 and molecular weight markers are indicated.

lowing the cell lysis. Further, ELISA tests revealed loss of conformational epitopes, indicating that BBA VP7 was not folded correctly. At the junction site, BBA VP7 has an arginine replacing an isoleucine residue (I251), which may have disrupted the protein structure similar to the previously reported substitution of a conserved lysine (K255) by leucine in BTV-10 VP7 (LeBlois and Roy, 1993). In the case of BBA VP7, it is likely that the insolubility was due to disruption of helical contacts within the core of the bottom domain rather than the result of an individual aa change. This view is further supported by the data obtained from an additional chimeric molecule, ABB. In this construct, the N terminal region (aa 1 to 120) encompasses AHSV-4 VP7 and the remaining molecule (aa 121 to 349) consists of BTV-10 VP7. Although ABB does not possess any mutated residues as in the case of BBA, nevertheless, correct folding was also disrupted.

In other studies it has been reported that single amino acid substitutions can significantly improve protein solubility (Zhao and Sommerville, 1992; Izard *et al.,* 1994; Jenkins *et al.,* 1996). Based on the available crystallographic data, A167 and F209 have been proposed as candidates for mutations to increase the solubility of AHSV-4 VP7. The arginine at aa position 168 of BTV-10 VP7 forms part of an RGD motif, implicated in cellular attachment of bluetongue cores, similarly to the foot and mouth disease virus where the RGD site is involved in attachment to an integrin receptor (Fox *et al.,* 1989; Logan *et al.,* 1993; Mason *et al.,* 1994). The mutations were carried out both in the wild-type AHSV VP7 and chimeric BAB VP7 and were shown to have a more pronounced effect in case of BAB VP7. Both mutated BAB7-A167R and BAB7-F209T proteins were recovered in the supernatant following lysis of infected cells with nonionic detergent. Mapping the hydrophobicity plots to the solvent-accessible surface of BTV-10 VP7 trimers have shown the presence of a large hydrophilic area composed of strand βC and η1 (aa 168–176, including the RGD motif) of the top domain of one monomer, and the C-terminal helix 9 of the adjoining monomer (Basak *et al.,* 1996). R168, which in AHSV is replaced by A167, forms part of this area. The lower solubility of AHSV VP7 mutant A167R compared with the same mutation in the chimeric BAB VP7 might reflect the impact of the C-terminal helix 9, as the C-terminus of AHSV VP7 is more hydrophobic with L346 replacing R345 of BTV VP7.

The related BTV-10 and AHSV-4 VP7 proteins have only 45% identity. Nevertheless, replacement of entire domains was successful between these proteins. The chimeric VP7 proteins folded correctly and retained the epitopes of the respective domains. Analysis of the effects of substitution of helices within the bottom domain have, however, revealed that such mutations interfered with protein folding, indicating that the interdomain amino acids interactions are very specific. ABA VP7 crystallization trials are underway to determine the structure of the bottom domain. These data should indicate which amino acid residues of the AHSV-4 VP7 protein interact with the AHSV VP3 scaffold and open up the opportunity for precise mapping of such residues by site-directed mutagenesis.

ACKNOWLEDGMENTS

We are grateful to Prof. D. Stuart and Dr. P. Gouet for helpful discussions and permission to use the data shown in Fig. 1A. We thank Drs. W. Jiang and E. Gould for raising the anti-BTV-10 VP7 MAbs. We are grateful to Drs. I. Casal and J. Martinez-Torrecuadrada (INGENASA, Spain) for providing us with anti-AHSV-4 VP7 MAbs. This work was funded by grants from MRC and BBSRC.

REFERENCES

Basak, A. K., Stuart, D. I., and Roy, P. (1992). Preliminary crystallographic study of bluetongue virus capsid protein, VP7. *J. Mol. Biol.* 228, 687–689.

Basak, A. K., Gouet, P., Grimes, J., Roy, P., and Stuart, D. (1996). Crystal structure of the top domain of African horsesickness virus VP7: Comparisons with bluetongue virus VP7. *J. Virol.* 70, 3797–3806.

Brown, M., and Faulkner, P. (1977). A plaque assay for nuclear polyhedrosis viruses using a solid overlay. *J. Gen. Virol.* 36, 361–364.

Burroughs, J. N., O'Hara, R. S., Smale, C. J., Hamblin, C., Walton, A., Armstrong, R., and Mertens, P. P. C. (1994). Purification and properties of virus particles, infectious subviral particles, cores and VP7 crystals of African horsesickness virus serotype 9. *J. Gen. Virol.* 75, 1849–1857.

Burroughs, J. N., Grimes, J. M., Mertens, P. P. C., and Stuart, D. (1995). Crystallisation and preliminary X-ray analysis of the core particle of bluetongue virus. *Virology* 210, 217–220.

Chuma, T., Le Blois, H., Sanchez-Vizcaino, J. M., Diaz-Laviada, M., and Roy, P. (1992). Expression of the major core antigen VP7 of African horsesickness virus by a recombinant baculovirus and its use as a group-specific diagnostic reagent. *J. Gen. Virol.* 73, 925–931.

Clapp, L. L., and Patton, J. T. (1991). Rotavirus morphogenesis: domains in the major inner capsid protein essential for binding to single-shelled particles and for trimerisation. *Virology* 180, 697–708.

Felgner, P. L., Gadek, T. R., Holm, M., Roman, R., Chan, H. W., Wenz, H., Northrop, J. P., Ringold, G. M., and Danielsen, M. (1987). Lipofection: A highly efficient, lipid-mediated DNA-transfection procedure. *Proc. Natl. Acad. Sci. USA* 84, 7413–7417.

Fox, G., Parry, N. R., Barnett, P. V., McGinn, B., Rowlands, D. J., and Brown, F. (1989). The cell attachment site on foot-and-mouth disease virus includes the amino acid sequence RGD (Arginine-Glycine-Aspartic acid). *J. Gen. Virol.* 70, 625–637.

French, T. J., and Roy, P. (1990). Synthesis of bluetongue virus (BTV) corelike particles by a recombinant baculovirus expressing the two major structural core proteins of BTV. *J. Virol.* 64, 1530–1536.

Gould, E. A., Buckley, A., and Cammack, N. (1985). Use of the biotin-streptavidin interaction to improve flavivirus detection by immunofluorescence and ELISA tests. *J. Virol. Methods* 11, 41–48.

Grimes, J., Basak, A. K., Roy, P., and Stuart, D. (1995). The crystal structure of bluetongue virus VP7. *Nature* 373, 167–170.

Hewat, E. A., Booth, T. F., and Roy, P. (1992a). Structure of bluetongue virus particles by cryo-electron microscopy. *J. Struct. Biol.* 109, 61–69.

Hewat, E. A., Booth, T. F., Loudon, P. T., and Roy, P. (1992b). 3D reconstruction of bluetongue virus core-like particles by cryo-electron microscopy. *Virology* 189, 10–20.

Hewat, E. A., Booth, T. F., and Roy, P. (1994). Structure of correctly self-assembled bluetongue virus-like particles. *J. Struct. Biol.* 112, 183–191.

Iwata, H., Chuma, T., and Roy, P. (1992a). Characterization of the genes encoding two of the major capsid proteins of epizootic haemorrhagic disease virus indicates a close genetic relationship to bluetongue virus. *J. Gen. Virol.* 73, 915–924.

Iwata, H., Yamagawa, M., and Roy, P. (1992b). Evolutionary relationships among the gnat-transmitted orbiviruses that cause African horsesickness, bluetongue and epizootic haemorrhagic disease as evidenced by their capsid protein sequences. *Virology* 191, 251–261.

Izard, J., Parker, M. W., Chartier, M., Duche, D., and Baty, D. (1994). A single amino acid substitution can restore solubility of aggregated colicin A mutants in *Escherichia coli. Protein Eng.* 7, 1495–1500.

Jenkins, T. M., Enlgeman, A., Ghirlando, R., and Craigie, R. (1996). A soluble active mutant of HIV-1 integrase: involvement of both the core and carboxy-terminal domains in multimerisation. *J. Biol. Chem.* 271, 7712–7718.

Kimura-Kuroda, J., and Yasui, K. (1983). Topographical analysis of antigenic determinants on envelope glycoprotein V3 (E) of Japanese encephalitis virus using monoclonal antibodies. *J. Virol.* 45, 124–132.

King, L. A., and Possee, R. D. (1992). "The Baculovirus Expression System: A Laboratory Guide." Chapman & Hall, London.

Kitts, P. A., and Possee, R. D. (1993). A method for producing recombinant baculovirus expression vectors at high efficiency. *BioTechniques* 14, 810–817.

Kunkel, T. A., Roberts, J. D., and Zakuor, R. A. (1987). Rapid and efficient method of site-specific mutagenesis without phenotypic selection. *Methods Enzymol.* 154, 367–382.

LeBlois, H., Fayard, B., Urakawa, T., and Roy, P. (1991). Synthesis and characterization of chimeric particles between epizootic haemorrhagic disease virus and bluetongue virus: Functional domains are conserved on the VP3 proteins. *J. Virol.* 65, 4821–4831.

LeBlois, H., and Roy, P. (1993). A single point mutation in the VP7 major core protein of Bluetongue virus prevents the formation of core-like particles. *J. Virol.* 67, 353–359.

Livingstone, C., and Jones, I. M. (1989). Baculovirus expression vector with single-strand capability. *Nucleic Acids Res.* 17, 2366.

Logan, D., Abu-Ghazaleh, R., Blakemore, W., Curry, S., Jackson, T., King, A., Lea, S., Lewis, R., Newman, J., Parry, N., Rowlands, D., Stuart, D., and Fry, E. (1993). Structure of a major immunogenic site on foot-and-mouth disease virus. *Nature* 362, 566–568.

Mason, P. W., Reider, E., and Baxt, B. (1994). RGD sequence of foot-and-mouth disease virus is essential for infecting cells via the natural receptor but can be bypassed by an antibody-dependent enhancement pathway. *Proc. Natl. Acad. Sci. USA* 91, 1932–1936.

Matsuura, Y., Possee, R. D., Overton, H. A., and Bishop, D. H. (1987). Baculovirus expression vectors: The requirements for high level expression of proteins, including glycoproteins. *J. Gen. Virol.* 68, 1233–1250.

Murphy, F. A., Borden, E. C., Slope, R. E., and Harrison, A. (1971). Physicochemical and morphological relationships of some arthropod-borne viruses to bluetongue virus — A new taxonomic group. Electron microscopic studies. *J. Gen. Virol.* 13, 273–288.

Oldfield, S., Adachi, A., Urakawa, T., Hirasawa, T., and Roy, P. (1990). Purification and characterization of the major group-specific core antigen VP7 of bluetongue virus synthesized by a recombinant baculovirus. *J. Gen. Virol.* 71, 2649–2656.

Prasad, B. V. V., Yamaguchi, S., and Roy, P. (1992). Three-dimensional structure of single-shelled BTV. *J. Virol.* 66, 2135–2142.

Roy, P., Hirasawa, T., Fernandez, M., Blinov, V. M., and Sanchez-Vixcaino Rodrique, J. M. (1991). The complete sequence of the group-specific antigen, VP7, of African horsesickness virus serotype 4 reveals a close relationship to bluetongue virus. *J. Gen. Virol.* 72, 1237–1241.

Roy, P. (1996a). Orbivirus structure and assembly. *Virology* 216, 1–11.

Roy, P. (1996b). Orbiviruses and their replication. *In* "Fields Virology," 3rd ed., Chap. 56, pp. 1709–1734. Lippincott-Raven, Philadelphia, PA.

Sanger, J. A., Nicklen, S., and Coulson, A. R. (1977). DNA sequencing with chain-terminating inhibitors. *Proc. Natl. Acad. Sci. USA* 74, 5463–5467.

Zhao, G. P., and Sommerville, R. L. (1992). Genetic and biochemical characterization of the trpB8 mutation of Escherichia coli tryptophan synthase: An amino acid switch at the sharp turn of the trypsin-sensitive "hinge" region diminishes binding and alters solubility. *J. Biol. Chem.* 267, 526–541.